

1.5 URBAN GROWTH AND AEROSOL EFFECTS ON CONVECTION OVER HOUSTON

Gustavo G. Carrió, William Y. Cheng, William R. Cotton and Stephen M. Saleeby
Department of Atmospheric Science, Colorado State University, Fort Collins, Colorado

1. INTRODUCTION

Houston is one of the fastest growing metropolitan areas in the United States during the past three decades. In this study, we investigate the effects of the Houston metropolitan area on the characteristics and intensity of convection and precipitation, focusing on events triggered by the sea breeze circulation. For this purpose, we implemented the Town Energy Budget (TEB) urban model into the Regional Atmospheric Modeling System developed at Colorado State University (RAMS@CSU, Pielke et al., 1992; Cotton et al., 2003). TEB is now coupled to run in parallel as to maximize the full potential of our computing resources.

The Landsat Thematic Mapper™ National Land Cover Data (NLCD) for the Houston area corresponding to the years 1992, 2001, and 2006 were used as benchmarks for the experimental design of the land-use sensitivity experiments, including a run with "no city".

We focused on a convective storm triggered by the sea breeze circulation (Aug 24 2001) Sensitivity experiments with the different land use data sets were compared. Results indicated that land-use changes in the Houston area dramatically affected precipitation. Additional numerical experiments were performed considering aerosol sources linked to the urban cells concentration.

2. METHODOLOGY

2.1 The Atmospheric Model

RAMS@CSU was configured to use three two-way interactive nested model grids with 42 vertical levels and horizontal grid spacings of 15.0, 3.75, and 0.75 km centered over Houston.

Grid 1 (71X 61 grid points) and Grid 2 (102X102 grid points) were used to simulate the synoptic and mesoscale environments, respectively. While Grid 3 (202X202 grid points) was used to resolve deep convection as well as the sea breeze circulation. Figure 1 gives the location of these grids.

RAMS@CSU uses the two-moment bulk microphysics scheme (Meyers et al., 1997; Saleeby and Cotton, 2004). This version considers the explicit activation of CCN (and giant CCN), a bimodal representation of cloud droplets, and a bin-emulation approach for: droplet collection, ice-particle riming, and sedimentation, and direct radiative effects of aerosols.

The mixing ratios and number concentrations of all water species (cloud droplets, drizzle drops, rain, pristine ice, snow, aggregates, graupel and hail) were predicted. CCN, GCCN and IFN concentrations were also considered as prognostic variables.

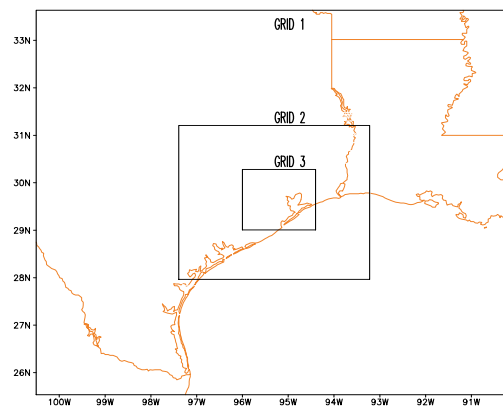


Figure 1: Location of grids 1, 2 and 3 used in the sensitivity experiment described in this abstract.

2.2 Experimental Design

We considered the NLCD corresponding to the Houston area as benchmarks for the experimental design of the land-use sensitivity experiments. One of the numerical experiments used the satellite data closest to the case we used for this study (2001), although, the urban cells were replaced by the predominant land use categories in the city surroundings (NO CITY). We considered aerosol observations during the

* Corresponding author address: Gustavo Gabriel Carrió, Department of Atmospheric Science, Colorado State University, Fort Collins, CO 80523; email: carriog@atmos.colostate.edu.

TexAQS/GoMACCS field campaign for the initialization CCN profiles. However, we eventually used lower CCN concentrations to characterize the city aerosol sources over each urban area. Increasing the latter above 2000cm^{-3} did not produce a significant impact on the results. In addition to high CCN concentrations over the city, we initialized the surroundings and the gulf area with more moderate values and cleaner air, respectively. These CCN concentrations were varied independently and simultaneously as shown in Table I.

LANDUSE	CCN concen [cm^{-3}]		
	CITY	BACKGROUND	GULF
1992	1500	500	150
NLCD	2000	800	200
2001	1500	500	150
NLCD	2000	800	200
2006	1500	500	150
NLCD	2000	800	200
NO CITY		500	150
		800	200

Table I: Performed numerical experiments. Red numbers correspond to results presented in this abstract

3. SUMMARY OF RESULTS

3.1 Urban size runs

Figure 2 compares maps of maximum updrafts for different scenarios: NO CITY, and considering 1992, 2001, and 2006 land use satellite data. Cells covered a larger area for “larger cities”, although updraft intensity did not show a regular behavior. Conversely, downdrafts tended to be stronger for larger urban areas (not shown). The latter result could be linked to the higher number of convective cores that develop.

The intensity of the sea-breeze (~SE) increased monotonically for larger urban areas. The intensity of flux averaged over the first km is compared in figure 3 for 2001 and 2006 runs. These plots correspond to a time one hour before the most intense activity occurred (~ 18:30Z).

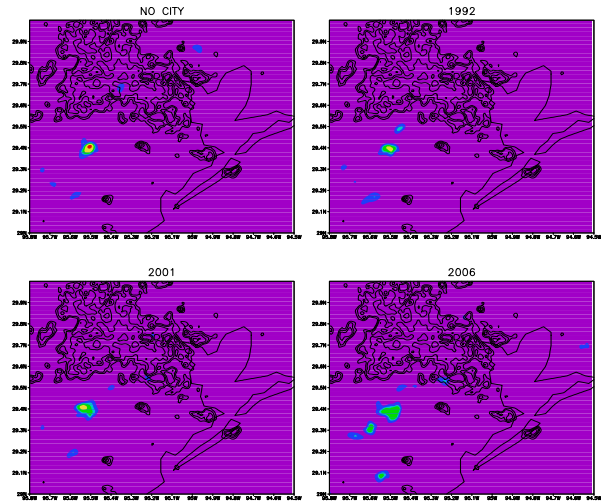


Figure 2: Maximum updraft for runs that only vary the city size.

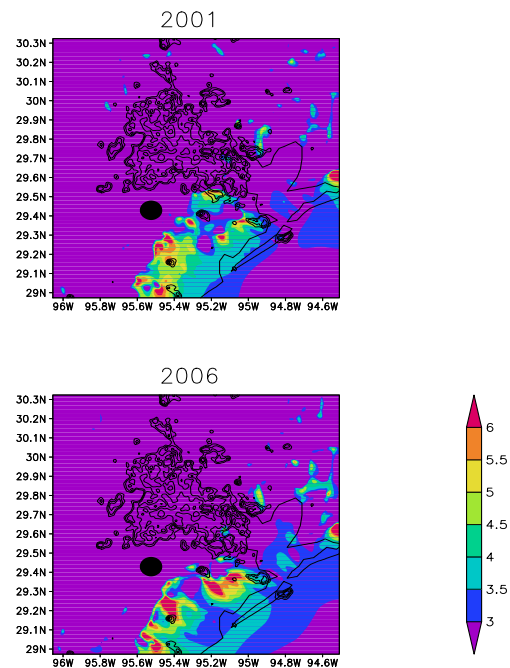


Figure 3: Flux along the direction of the sea breeze, averaged over the first km [$\text{Kg m}^{-2}\text{s}$]

Varying the city size exhibited a significant impact on precipitation. Precipitation rates as well as the total volume of precipitated water monotonically increased when considering larger urban areas (see Figure 4). The **NO CITY** run exhibits a maximum rate much later. Total volume of precipitation, integrated over the finest grid

increased monotonically 9, 11, and 30% (over **NO CITY**) for **1992**, **2001**, and **2006**, respectively.

were less important, and precipitation rates did not show a monotonic behavior.

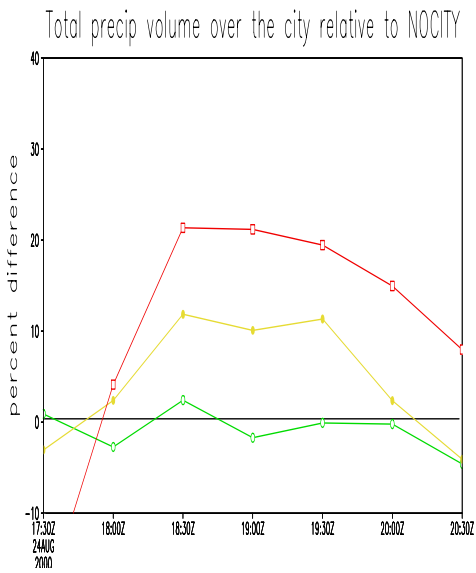
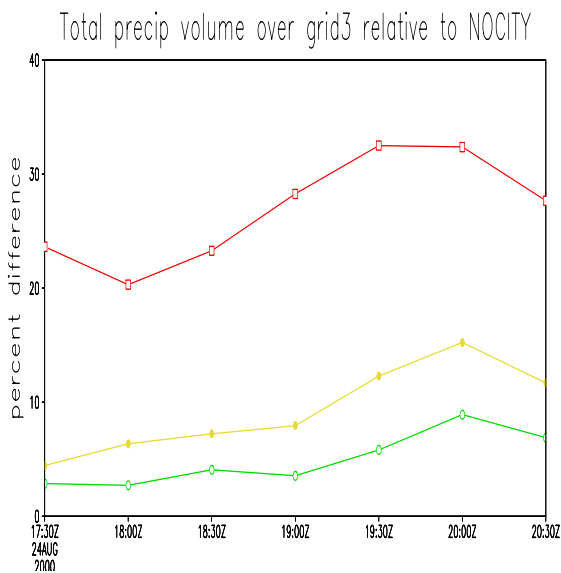
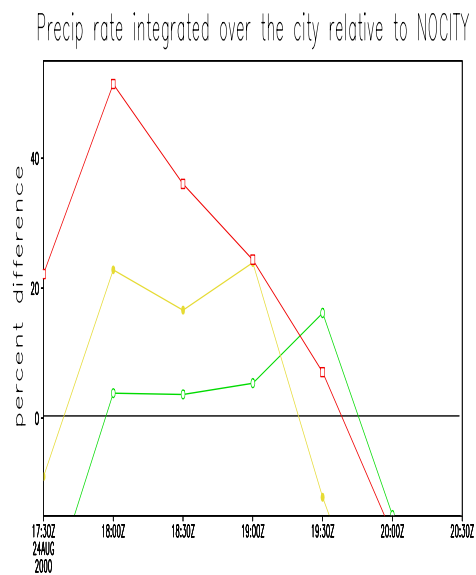
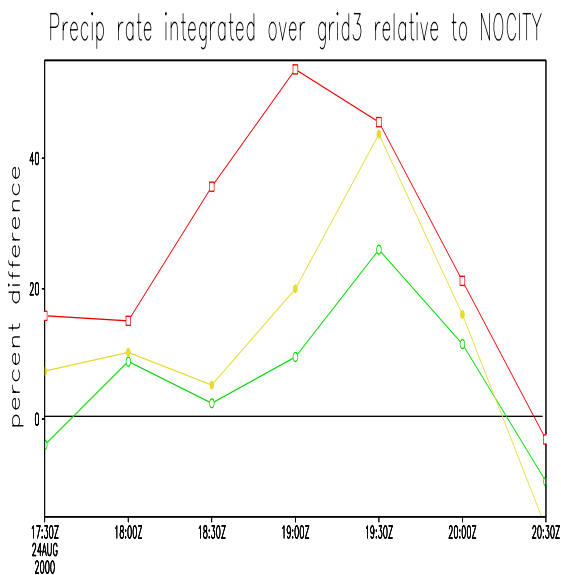


Figure 4: Time evolution of the precipitation rates (a) and total volume of the precipitated water (b). The curves represent values integrated over the finest grid (grid 3) and relative to the NO CITY run. Green, yellow, and red denote 1992, 2001, and 2006 runs, respectively

Figure 5: Idem Figure 4 but just for the urban area.

Varying the size of the city had no impact on the liquid water content (LWC) maxima as seen in Figure 6a. Relative differences in LWC are very small for the period of intense convection (~18:30Z).

Figure 5 is analogous to figure 4 although considers only the urban area. In this case, differences in the total volume of precipitated water

However, large relative differences correspond to integral value of the condensed mass, mainly due to a larger area covered by the convective cores.

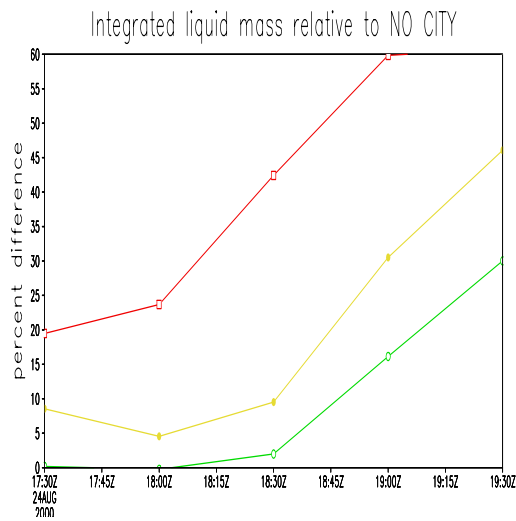
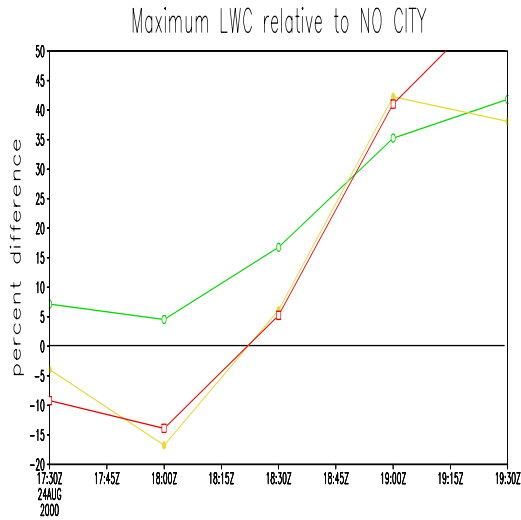


Figure 6: Time evolution of the LWC maxima (a) and total mass of condensed water (b). The curves represent values integrated over the finest grid (grid 3) and relative to the NO CITY run. Green, yellow, and red denote 1992, 2001, and 2006 runs, respectively.

3.1 Aerosol runs

As mentioned in Section 2.2, air over the gulf, the urban area, and the rest of the land grid cells in grids 2 and 3 were initialized with CCN profiles corresponding to clean, moderate, and polluted environments, respectively. It must be noted that during the simulations (high) CCN concentrations were nudged over the cities to consider the aerosol sources.

For this case, the effect of considering more polluted cities on precipitation was a much less important. Figure 7 compares the evolution of the total mass of precipitated water for three runs initialized with different CCN concentrations over the urban area 1500 and 2000cm^{-3} , and 300cm^{-3} (clean city)

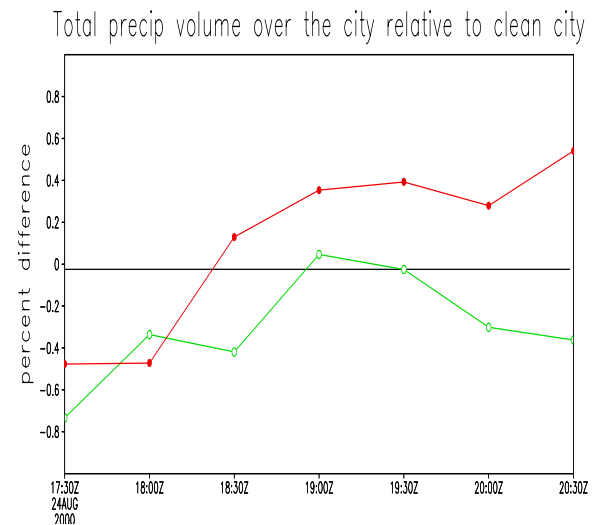
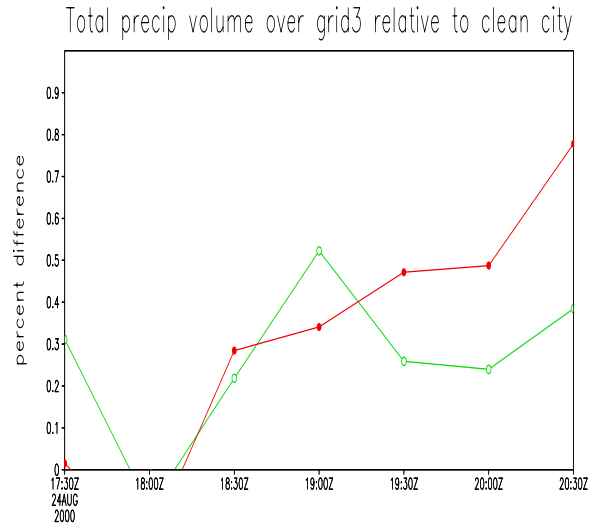


Figure 7: Time evolution of the total mass of precipitated water for (a) the entire grid 3, and (b) just the urban area. The curves represent values relative to the clean city run with 2001 land use. Green and red denote 1500 and 2000cm^{-3} , respectively.

Differences integrated over the entire Grid 3 were small although positive. However, values integrated over the urban area did not show a regular behavior.

Conversely, the effects of enhancing aerosol concentrations over the urban area on the microphysics were more. Figure 8 is analogous to Fig 7 but compares LWC maxima and the integral mass values of condensed liquid water. Enhancing aerosols increased the maximum values of LWC simulated over Grid 3 during the period of intense convection (~ between 18:00-19:00Z). Higher values of total liquid water mass integrated over grid 3 were simulated for more polluted cities (Fig7b).

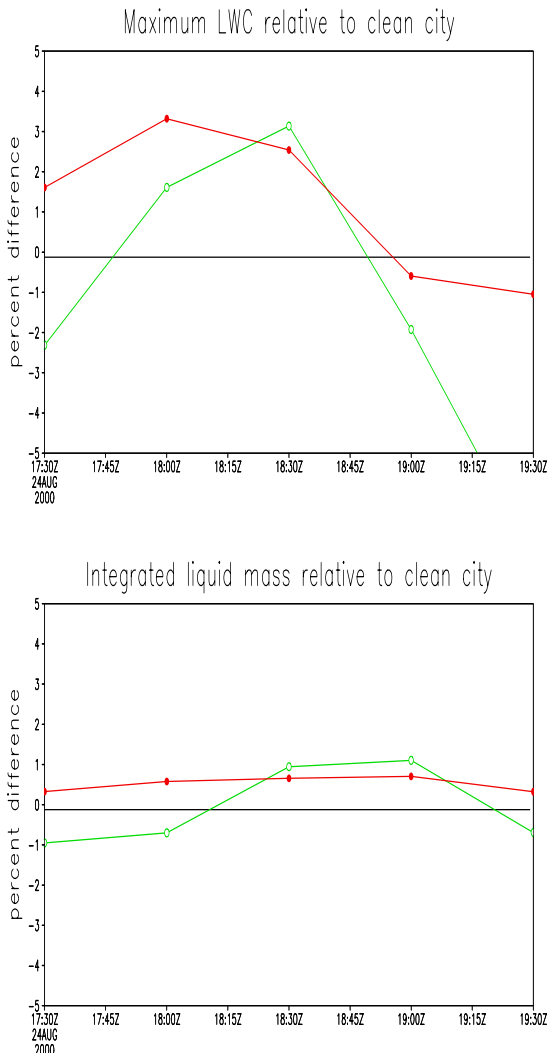


Figure 7: Time evolution of (a) LWC maxima, and (b) the total mass of liquid water. The curves represent values relative to the clean city run (all runs with 2001 land use). Green and red denote 1500 and 2000 cm^{-3} , respectively.

When comparing the supercooled water paths between -10 and -20°C (in this case,

approximately between 4000 and 8000m of altitude), the values simulated for 1500 and 2000 cm^{-3} were 4 and 9% (respectively) higher than those of the clean city (not shown). Maximum ice water paths (IWPs) also increased when considering more intense sources over the city (not shown)

4. CONCLUSIONS

We examined the effect of Houston's urban growth on convection/precipitation using realistic benchmarks for the land use changes (i.e., 1992, 2001, and 2006 satellite data). We used RAMS@CSU coupled to the Town Energy Budget (TEB) generalized canyon model and, in the present study, we focused on a convective case occurred in Houston on August 24 2000.

In summary, considering "larger cities", we simulated:

- higher precipitation rates over the finest grid, the NO CITY run exhibits a maximum much later,
- the precipitation rates and accumulated values over urban cells showed lower but positive differences,
- increased intensity of the sea breeze,
- total volume of precipitation (finest grid) increased monotonically 9, 11, and 30% (over NOCITY) for 1992, 2001, and 2006, respectively,
- LWPs and updrafts maxima did not change significantly,
- conversely, the integral value of condensate and maximum downdrafts increased. The latter result is linked to the larger area coverage of the storm.

While "more polluted cities" resulted in:

- positive differences in LWC maxima for the period of intense convection (~18:00-19:00Z),
- +4% and +9% difference for supercooled water between -10 and -20°C (~4-8km). It is well known that presence of supercooled liquid water within this temperature range plays an important role in non-inductive charge separation mechanisms,
- differences in the total precipitated volume are really small for both domain and the city, although positive for the first,
- maximum IWPs also increased when considering more intense sources over the city.

Previous research (e.g. Albrecht 1989; Kaufman and Nakajima 1993; Borys et al. 1998; Rosenfeld 1999, 2000; Andreae et al. 2004) indicated that increases in CCN number concentrations tend to reduce warm rain efficiencies and increase cloud water contents. In addition greater amounts of supercooled water will be available enhancing non-inductive charge separation mechanisms.

Enhancing CCN concentrations has also been found to increase the mass transported out of the storm through the outflow (Van den Heever et al 2006; Carrió et al, 2007). After a few hours of evolution, the anvil clouds have narrower ice particle size distributions characterized by higher frequencies for smaller ice particles that lead to an increased cloud lifetime (Carrió et al, 2007). Some preliminary results suggest a similar behavior for anvil cirrus clouds generated by the studied storm. For this purpose, we will run two experiments with different urban aerosol concentration with a much longer simulation time.

As mentioned in Section 4, the effects of the city size on precipitation are dominant for the examined case. Finally, we plan to perform a similar series of simulations for a more synoptically-forced Houston storm.

5. ACKNOWLEDGEMENTS

The authors want to thank NOAA for financial support (NA07OAR4310281).

6. REFERENCES

- Albrecht, B., 1989: Aerosols, cloud microphysics, and fractional cloudiness. *Science*, **245**, 1227-1230.
- Andreae, M.O., D. Rosenfeld, P. Artaxo, A.A. Costa, G.P. Frank, K.M. Longo, and M.A.F. Silva-Dias, 2004: Smoking rain clouds over the Amazon. *Science*, **303**, 1337-1342.
- Borys, R.D., D.H. Lowenthal, M.A. Wetzal, F. Herrera, A. Gonzalez, and J. Harris, 1998: Chemical and microphysical properties of marine stratiform cloud in the North Atlantic. *J. Geophys. Res.*, **103**, 22,073-22,085.
- Carrió, G. G., S. van den Heever, and W. R. Cotton, 2007: Impacts of nucleating aerosol on anvil-cirrus clouds: A modeling study. *Atmos. Res.*, **84**, 111-131.
- Cotton, W.R., R.A. Pielke Sr., R.L. Walko, G.E. Liston, C.J. Tremback, H. Jiang, R.L. McAnelly, J.Y. Harrington, M.E. Nicholls, G.G. Carrió, and J.P. McFadden, 2003: RAMS 2001: Current status and future directions. *Meteor. Atmos. Phys.*, **82**, 5-29.

- Kaufman, Y.J., and T. Nakajima, 1993: Effect of Amazon smoke on cloud microphysics and albedo-analysis from satellite imagery. *J. Appl. Meteor.*, **32**, 729-744.
- Meyers, M.P., R.L. Walko, J.Y. Harrington, and W.R. Cotton., 1997: New RAMS cloud microphysics parameterization. Part II: The two-moment scheme. *Atmos. Res.*, **45**, 3-39.
- Pielke, R.A., W.R. Cotton, R.L. Walko, C.J. Tremback, W.A. Lyons, L.D. Grasso, M.E. Nicholls, M.D. Moran, D.A. Wesley, T.J. Lee, and J.H. Copeland, 1992: A comprehensive meteorological modeling system – RAMS. *Meteor. Atmos. Phys.*, **49**, 69-91.
- Rosenfeld, D., 1999: TRMM observed first direct evidence of smoke from forest fires inhibiting rainfall. *Geophys. Res. Lett.*, **26**, 3105-3108.
- Rosenfeld, D., 2000: Suppression of rain and snow by urban and industrial air pollution. *Science*, **287**, 1793-1796.
- Saleeby, S.M., and W.R. Cotton, 2004: A large-droplet mode and prognostic number concentration of cloud droplets in the Colorado State University Regional Atmospheric Modeling System (RAMS). Part I: Module descriptions and supercell test simulations. *J. Appl. Meteor.*, **43**, 182-195.
- van den Heever, S.C., Carrió, G. G., Cotton, W. R., DeMott, P. J. and A. J. Prenni, 2006. Impacts of nucleating aerosol on Florida convection. : Mesoscale simulations. *J. Atmos. Sci*, **63**, 1752-1775.